

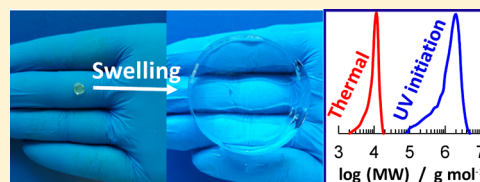
A Self-Healing and Highly Stretchable Polyelectrolyte Hydrogel via Cooperative Hydrogen Bonding as a Superabsorbent Polymer

Esra Su, Mine Yurtsever,^{1b} and Oguz Okay*^{1b}

Department of Chemistry, Istanbul Technical University, Maslak, 34469 Istanbul, Turkey

S Supporting Information

ABSTRACT: Poly(2-acrylamido-2-methyl-1-propanesulfonic acid) (PAMPS) hydrogels are attractive materials for various application areas due to their pH-independent large swelling capacities. However, their covalently cross-linked network structure leads to a brittle behavior even at low strains. We present here for the first time highly stretchable superabsorbent PAMPS hydrogels formed via H-bonds entirely that are stable in water. UV polymerization of AMPS in aqueous solutions at 23 ± 2 °C without a chemical cross-linker produces hydrogels with large swelling capacities exceeding 1000 times their original mass. Although the hydrogels are stable in water, they easily dissolve in chaotropic solvents, suggesting that they form via H-bonding interactions between PAMPS chains. We show that the high molecular weight of the primary chains of PAMPS hydrogels formed via UV polymerization contributes to the H-bonding cooperativity and hence is responsible for their stability in water. Incorporation of *N,N*-dimethylacrylamide (DMAA) segments into the physical PAMPS network further increases the molecular weight of the primary chains, leading to enhanced mechanical strength of the hydrogels. PAMPS/DMAA hydrogels in their as-prepared states exhibit a high modulus (up to 0.41 MPa), tensile fracture stress (up to 0.57 MPa), and high stretchability ($\sim 1000\%$) together with an extraordinary swelling capacity (up to ~ 1700 g g⁻¹) and complete self-healing efficiency.



INTRODUCTION

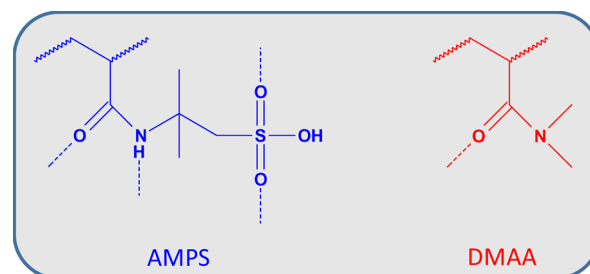
The classical first-generation hydrogels are chemically cross-linked hydrophilic polymers absorbing large quantities of water while maintaining their integrity.¹ Although such hydrogels display spectacular features offering a wide range of potential application areas, they encounter irreversible damage under low strain due to the absence of an efficient mechanism for energy dissipation.^{2,3} To overcome this limitation, several studies in the last decade have focused on preparing mechanically strong physically cross-linked hydrogels.⁴ Although physical hydrogels can easily be prepared via noncovalent interactions such as H-bonding^{5–10} or hydrophobic interactions,^{11–13} they generally exhibit insufficient mechanical strength or low water holding capacity due to the weak intermolecular bonds. Considering the strength of H-bonds is about 100-fold weaker than that of the covalent bonds, generation of a strong physically cross-linked polymer or gel requires H-bonding cooperativity.^{14,15} Such a strengthening effect of the cooperativity of H-bonds is observed in nature, starting from water molecules up to biopolymers such as double-stranded DNA or proteins.¹⁶ For instance, the stability of the secondary and tertiary structures of proteins and DNA arises from the cooperative effect of H-bonds between the oxygen atom of the C=O and NH fragments, acting as a proton acceptor and donor, respectively.

The general strategy for the preparation of mechanically strong hydrogen-bonded hydrogels is to reduce their water contents and hence amplify H-bonding interactions.^{17–25} For instance, hydrogen-bonded physical hydrogels with moderate water contents (30–80%) were prepared using dual amide

groups,¹⁷ diaminotriazine–diaminotriazine interactions,^{18,19} ureidopyrimidinone units,^{20,21} and H-bond acceptor and donor comonomer units.^{22–25} To our knowledge, superabsorbent hydrogels formed via H-bonds entirely that are stable in water with a swelling capacity exceeding 1000 times their original mass have not been reported before.

2-Acrylamido-2-methyl-1-propanesulfonic acid (AMPS) is a popular strong electrolyte monomer widely used in the preparation of superabsorbent polymers exhibiting pH-independent large swelling capacity (Scheme 1).^{26–31} Poly-(AMPS) (PAMPS) hydrogels are also attractive materials in bioengineering, food industry, agriculture, and water purification.^{32–36} However, because PAMPS hydrogels have generally

Scheme 1. Structure of AMPS and DMAA Monomer Units^a



^aDashed lines represent H-bonding regions.

Received: January 7, 2019

Revised: April 9, 2019

Published: April 22, 2019

Table 1. Compositions, Swelling and Mechanical Properties of Hydrogels^a

code	C ₀ /%	x _{DMAA}	m _{rel}	H ₂ O%	W _g	E/kPa	tensile		compression	
							σ _f /kPa	ε _f %	σ _f /MPa	ε _f %
T-50	50	0	soluble	soluble	0	9(2)	12(1)	2500(360)		
U-50	50	0	877(77)	99.94	1.00	27(2)	64(6)	1900(110)		
U-55	55	0	962(40)	99.95	0.93	39(3)	95(8)	1320(120)		
U-60	60	0	1013(53)	99.94	0.99	65(5)	114(7)	1120(90)	9(0.3)	95
U-70/0.5	70	0.46	1662(11)	99.99	1.11	172(8)	303(13)	1130(40)	12(0.4)	93
U-75/0.6	75	0.62	1026(67)	99.99	1.13	407(22)	568(40)	1010(80)	14(1.3)	89
U-80/0.7	80	0.74	934(40)	99.99	1.11	372(14)	518(27)	1020(70)		

^aStandard deviations are given in parentheses. They are less than 5% for m_{rel}, W_g, and ε_f values.

been prepared via covalent cross-links, they exhibit poor mechanical properties, limiting their application areas. Recent work shows that AMPS undergoes spontaneous initiator-free thermal polymerization in concentrated aqueous solutions at elevated temperatures leading to the formation of physical PAMPS hydrogels.^{37,38} The resulting physical gels formed via H-bonds between carbonyl and amino groups of AMPS units are highly stretchable (up to 2500% stretch at break), but they exhibit poor mechanical properties and hence easily dissolve in aqueous media, suggesting weak H-bonding interactions between PAMPS chains.^{31,37} This is expected due to the strong polyelectrolyte nature of PAMPS in aqueous media, generating a high osmotic pressure exerted by the AMPS counterions. This osmotic pressure seems to dominate over the rubber-like elasticity of the physical PAMPS network leading to its disruption in water.

Here, we show that UV polymerization of AMPS at room temperature (23 ± 2 °C) without a chemical cross-linker leads to the formation of water-insoluble, highly stretchable hydrogels with large swelling capacities (up to 1013 ± 53 g·g⁻¹). Although the hydrogels are stable in water, they easily dissolve in chaotropic solvents, suggesting that they form via H-bonding interactions between PAMPS chains. The question arising is why UV-polymerized hydrogels are stable in water as compared to the water-soluble thermal-polymerized ones. In the following, we discuss and compare rheological and mechanical properties of PAMPS hydrogels prepared via UV and thermal polymerizations. As will be seen below, the molecular weight of PAMPS primary chains isolated from UV-polymerized hydrogels is around two orders of magnitude higher than that of thermal polymerized ones, which is responsible for their stability in water. We also hypothesized that the incorporation of *N,N*-dimethylacrylamide (DMAA) units into the physical PAMPS network would further enhance the mechanical strength of PAMPS hydrogels. Although DMAA units are unable to form H-bonds between one another due to their dimethyl amino groups, they exhibit enhanced proton acceptor properties of their C=O groups through the σ-donation effect of the methyl groups (Scheme 1). This would contribute to the cooperativity of H-bonds in PAMPS/DMAA hydrogels. We indeed observed that the addition of DMAA significantly improves both the mechanical and self-healing properties of physical PAMPS hydrogels in their as-prepared states without changing their high stretchability and extraordinary swelling capacity.

EXPERIMENTAL PART

Materials. 2-Acrylamido-2-methylpropane-1-sulfonic acid (AMPS, 99%, Sigma-Aldrich), *N,N*-dimethylacrylamide (DMAA, 99%, Sigma-Aldrich), 2-hydroxy-4'-(2-hydroxyethoxy)-2-methylpropiophenone Ir-

gacure 2959, 98%, Sigma-Aldrich), *N,N'*-methylenebis(acrylamide) (BAAM, 99%, Merck), and poly(ethylene glycol) (PEG, 10,000 g·mol⁻¹, Sigma-Aldrich) were used without purification.

Preparation of Hydrogels. Hydrogels were prepared by UV-initiated solution polymerization of AMPS at 23 ± 2 °C without and with DMAA in water using Irgacure 2959 as a photoinitiator. No chemical cross-linker was used in the gel preparation. The total monomer concentration C₀ was varied between 50–80 wt %, whereas the DMAA mole fraction x_{DMAA} in the comonomer mixture was changed between 0 and 0.74 (Table 1). To illustrate the synthetic procedure, we give details for the preparation of a hydrogel at C₀ = 75 wt %, x_{DMAA} = 0.62, and in the presence of 0.2 mol % Irgacure initiator (with respect to the monomers). AMPS (2.50 g) and DMAA (2.00 g) were first mixed and dissolved in 1.50 mL of distilled water at 35 °C to obtain a homogeneous solution. After stirring for 10 min under bubbling nitrogen gas, Irgacure 2959 (14 mg) was added, and the solution was transferred into plastic syringes of 20 mm in diameter and into rectangular plastic molds (20 cm × 1 cm) of 1 mm in thickness. The polymerization was conducted at 23 ± 2 °C for 24 h under UV light at 360 nm. For comparison, PAMPS hydrogels were also prepared by thermal polymerization of aqueous 50 wt % AMPS solutions at 80 °C in the absence of an external initiator, as described before.^{31,37}

Swelling Tests and Gel Fractions. The hydrogels prepared in the syringes were cut into specimens of ~3 mm in length and immersed in excess distilled water at 23 ± 2 °C for at least 2 weeks by replacing water several times to wash out any soluble polymers, unreacted monomers, and the initiator. After reaching swelling equilibrium, the specimens were taken out of water and freeze-dried (Christ Alpha 2-4 LDplus). The fraction of the monomers converted into a water-insoluble polymer, that is, the gel fraction W_g was calculated as W_g = m_{dry}/(10⁻²m₀C₀), where m₀ and m_{dry} are the masses of the specimen just after synthesis and after drying, respectively. The relative weight swelling ratio m_{rel} was calculated as m_{rel} = m/m₀, where m is the mass of the equilibrium swollen gel specimen. The water content H₂O% of the equilibrium swollen hydrogels was calculated as H₂O% = 10²(1 - m_{dry}/m).

Solubilization of the Hydrogels and Gel Permeation Chromatography (GPC) Measurements. PAMPS gel specimens (0.39 g) after preparation were solubilized in 100 mL of aqueous 5 M urea solution by stirring at room temperature for 5 days. For AMPS/DMAA copolymer hydrogels, complete solubilization of the specimens required 7 to 10 M urea solutions and a dissolution time of 15 days under stirring. The polymer solutions containing urea were then poured into dialysis tubes (3500 MWCO, SnakeSkin, Pierce) and dialyzed for 3 days against water that was changed 5 or 6 times. They were then further dialyzed for an additional 1 day against PEG-10000 to concentrate the solutions. The molecular weight of the polymers isolated from the hydrogels was estimated using GPC measurements conducted on an Agilent 1260 Infinity GPC equipped with Waters Ultrahydrogel 250 and 500 columns and a refractive index detector. A phosphate buffer (pH = 7, NaN₃ internal standard) at a flow rate of 0.7 mL·min⁻¹ was the mobile phase. Linear polyethylene oxide (PEO), polyethylene glycol (PEG) standards were used to assign molecular weights.

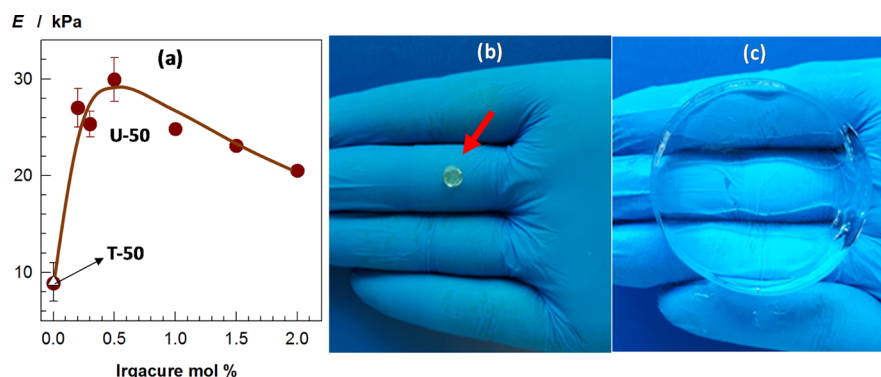


Figure 1. (a): Young's modulus E of U-50 gels plotted against Irgacure concentration. Open triangle represents the modulus of the T-50 gel. (b, c): Images of a U-60 gel specimen just after preparation (b) and after equilibrium swelling in water (c).

Rheological Experiments. The measurements were conducted at 25 °C on a Gemini 150 rheometer system, Bohlin Instruments, equipped with a solvent trap to prevent evaporation. The temperature was controlled with a Peltier system to maintain it constant at 25 °C. The gel specimens prepared in plastic molds were cut into thin slices of about 20 mm in diameter and 3 mm in thickness and then placed between the parallel plates of the rheometer. The upper plate (diameter: 20 mm) was set at a distance of $2950 \pm 150 \mu\text{m}$. The frequency sweep tests at a strain amplitude $\gamma_0 = 0.01$ were carried out over the frequency range 0.1 to 300 $\text{rad}\cdot\text{s}^{-1}$. The viscosities η of the polymer solutions isolated from the hydrogels were measured with a cone-and-plate geometry with a cone angle of 4° and diameter of 40 mm over the range of shear rates $\dot{\gamma} 2 \times 10^{-4}$ to $2 \times 10^3 \text{ s}^{-1}$. Zero-shear viscosities η_0 were estimated by fitting the viscosity data recorded at various shear rates to the Carreau model³⁹

$$\eta(\dot{\gamma}) = \eta_0 [1 + (\dot{\gamma}/\gamma_c)^2]^{-n/2} \quad (1)$$

where γ_c is the critical shear rate, and n is the shear thinning index of the shear thinning region.

Mechanical Tests. Uniaxial tensile and compression tests were performed on cylindrical and flat gel specimens, respectively, at 23 ± 2 °C using a Zwick Roell Z0.5 TH test machine with a 500 N load cell. The stress was presented by its nominal σ_{nom} and true values σ_{true} , which are the forces per cross-sectional area of the undeformed and deformed gel specimen, respectively. Assuming constant gel volume during deformation, the true stress σ_{true} was calculated as $\sigma_{\text{true}} = \lambda \sigma_{\text{nom}}$, where λ is the deformation ratio (deformed length/initial length). The strain ε is defined as the change in the length of the gel specimen relative to its initial length, that is, $\varepsilon = \lambda - 1$ or $1 - \lambda$, for elongation and compression, respectively. Young's modulus E was calculated from the slope of $\sigma_{\text{nom}} - \varepsilon$ curves between 5–15% deformations. For the tensile tests, the initial sample length between the jaws and the strain rate were $10 \pm 0.1 \text{ mm}$ and 1 min^{-1} , respectively. Cyclic tensile tests were conducted by stretching gel specimens at a strain rate $\dot{\varepsilon}$ of 5 min^{-1} to a maximum strain ε_{max} , followed by immediate retraction to zero displacement and a waiting time of 1 min until the next cycle of stretching. For the compression tests, the specimens were compressed at $\dot{\varepsilon} = 1 \text{ min}^{-1}$. The compressive fracture stress σ_f at failure was calculated from the maxima in true stress–strain curves, as detailed before.⁴⁰ For the determination of the self-healing ability of the hydrogels, cylindrical gel specimens of 4.6 mm in diameter and 9 cm in length were cut in the middle, and then the two halves were merged together within a plastic syringe of the same diameter as the specimen by slightly pressing the piston plunger. Tensile tests were performed on both healed and virgin gel specimens. Healing efficiencies ε_h were estimated from the ratio of the modulus, fracture stress, and fracture strain of the healed samples to those of the virgin ones. The healing time was varied between 0.25 and 72 h.

Quantum Mechanical Calculations (QMCs). QMCs were carried out to study the nature of H-bonds between AMPS monomers, (AMPS)₂, and AMPS/DMAA dimers in the gas phase

as well as in acidic aqueous medium with implicit and explicit water. The geometries of the studied systems were optimized by using DFT methodology at M062X/6-311+G(d,p) level of the theory. In the gas phase calculations, many conformations were generated, and only the data and figures belonging to the lowest energy structures were presented. The gas phase energies are the true minima confirmed by all positive frequencies. All the interaction energies are the basis set superposition error (BSSE)-corrected energies using a Counterpoise method obtained by single-point calculations at the same level of the optimizations. In acidic medium, each sulfonate ($-\text{SO}_3^-$) group carries a negative charge balanced by the proton, which is not naked but in the form solvated by a water molecule, H_3O^+ . To prevent hydrogen abstraction and preserve the electrostatic interactions between the sulfonate and hydronium ions, one more extra water molecule near the hydronium ion was added. All the dimeric systems were subjected to optimization at the same level of gas phase calculations in implicit water by adjusting the dielectric constant ε of the medium to 78. The solvent corrections were made using a standard IEFPCM model.

RESULTS AND DISCUSSION

UV versus Thermal Polymerization of AMPS. PAMPS hydrogels were synthesized by UV-initiated polymerization of aqueous AMPS solutions using Irgacure 2959 as the initiator without a chemical cross-linker. The concentration of AMPS at the gel preparation, C_0 , was varied from 50 wt % up to its solubility limit of 60 wt %. For comparison, thermal polymerization of AMPS at 80 °C without any initiator and cross-linker was also carried out. In the following paragraphs, PAMPS hydrogels formed via UV and thermal polymerizations are denoted as U- x and T- x gels, respectively, where x represents the AMPS concentration C_0 . Figure 1a shows the Young's modulus E of U-50 gels plotted against the initiator concentration. For comparison, the modulus of the T-50 gel is also shown by the open triangle. The modulus of the U-50 gel prepared in the absence of the UV initiator is $8.9 \pm 0.1 \text{ kPa}$, which is close to that of the T-50 gel ($9 \pm 2 \text{ kPa}$). Swelling tests showed that they both are easily soluble in water, suggesting weak intermolecular interactions. The modulus E rapidly increases with increasing initiator concentration, and after passing a maximum ($30 \pm 2 \text{ kPa}$) at around 0.5 mol % initiator, it starts to decrease continuously. All U-50 gels prepared in the presence of the initiator were stable in water for at least 8 months, and they all exhibited a gel fraction W_g close to unity, indicating that AMPS in the monomer feed was completely incorporated into the water-insoluble PAMPS network (Table 1). In the following, the initiator concentration was fixed at 0.2 mol % with respect to the monomer.

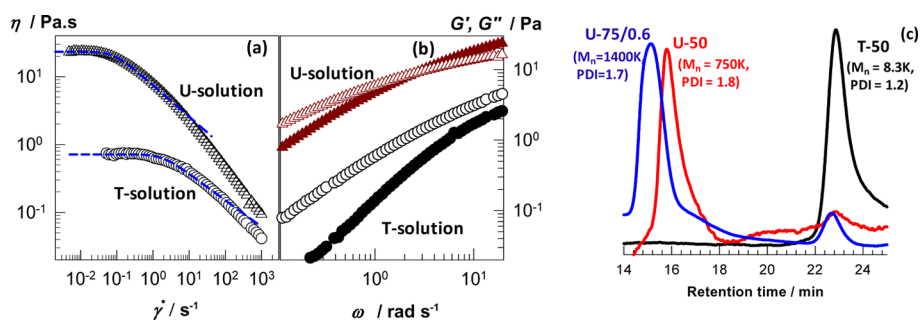


Figure 2. (a): Viscosities η of aqueous 0.39 wt % U-50 and T-50 solutions at 25 °C plotted against the shear rate $\dot{\gamma}$. The solutions were obtained from the corresponding hydrogels. The curves are the best fits to the Carreau model (eq 1) to estimate the zero-shear viscosity η_0 . (b): Frequency ω dependences of the storage G' (solid symbols) and loss moduli G'' (open symbols) of 0.39 wt % U- and T-solutions in water. $\gamma_0 = 0.1$; temperature = 25 °C. (c): GPC curves of the polymers isolated from U-50, T-50, and U-75/0.6 hydrogels, yielding \bar{M}_n values of 7.5×10^5 , 8.3×10^3 , and 1.4×10^6 g·mol⁻¹, with polydispersity indices of 1.8, 1.2, and 1.7, respectively.

All the U-gels exhibited large swelling capacities when immersed in water (Table 1). Figure 1b,c shows the images of a U-60 gel specimen just after preparation and after equilibrium swelling in water, respectively. The equilibrium weight swelling ratio m_{rel} of the hydrogel is 1013 ± 53 , indicating that the network chains are around 10-fold of stretched conformation as compared to their as-prepared states. m_{rel} slightly decreased with decreasing AMPS% and becomes 877 ± 77 at 50 wt % AMPS (Table 1, Figure S1).

Although U-gels are stable in water, they all could easily be dissolved in aqueous 5 M urea solution or in ethanol, which are known as chaotropic solvents disrupting H-bonds. This suggests that, similar to the T-gels, U-gels entirely form via hydrogen bonding interactions between PAMPS chains. To characterize the primary chains of the PAMPS network, we first dialyzed PAMPS/urea solutions isolated from the hydrogels against water for 3 days to remove urea, followed by dialyzing against aqueous PEG-10000 to concentrate the solutions. Figure 2a shows the shear rate $\dot{\gamma}$ dependence of the viscosities η of 0.39 wt % aqueous solutions of U-50 and T-50 obtained from the corresponding hydrogels. Both solutions exhibit a Newtonian plateau at low shear rates and start to shear-thin above a critical shear rate $\dot{\gamma}_c$. A U-50 solution has about 30-fold higher zero-shear viscosity η_0 than the T-50 solution (23.3 ± 0.1 vs 0.71 ± 0.01 Pa·s), revealing that the molecular weight of PAMPS is relatively high in the former solution. Figure 2b shows the angular frequency ω dependences of the storage G' (solid symbols) and loss moduli G'' (open symbols) of the same solutions. For the T-50 solution, G'' dominates over G' over the whole range of frequency, and hence it is a dilute polymer solution. In contrast, a viscoelastic spectrum of the U-50 solution is typical for a semi-dilute polymer solution, that is, G'' exceeds G' at low frequencies, and a crossover occurs between G' and G'' at a frequency of 2.6 rad·s⁻¹, corresponding to a characteristic time scale of 0.38 s for dissociation and association of noncovalent bonds. Frequency sweep tests conducted on hydrogels also show higher storage modulus G' and lower loss factor $\tan \delta$ ($\tan \delta = G''/G'$) of U-50 as compared to T-50 (Figure S2).

The molecular weight of PAMPS chains isolated from the hydrogels was determined via GPC analysis with PEO standards. The number-average molecular weight \bar{M}_n of the primary chains in U-gels was found to be much larger than that in T-hydrogels (Figure 2c). For instance, \bar{M}_n of the polymers isolated from U-50 is around 90-fold higher than that of T-50 (7.5×10^5 vs 8.3×10^3 g·mol⁻¹). Thus, we may attribute the

water stability of U-hydrogels to their longer PAMPS primary chains, providing formation of a larger number of H-bonds between two chains as compared to the water-soluble T-gels. Previous work indeed shows that the cooperativity of H-bonds becomes stronger as the degree of polymerization is increased.⁴¹ This behavior was attributed to the proximity effect of the already formed H-bonds between two long polymer chains, restricting the conformations of the chain segments and hence facilitating subsequent H-bond formation.^{42,43} We should mention that the H-bonds may also trap preexisting chain entanglements and hence increase their lifetimes to form chain-entanglement cross-links in the hydrogels. In addition, because the hydrophobic interactions and H-bonds can mutually reinforce each other,^{44,45} the hydrophobic alkyl part of AMPS units at a high concentration (50–60%) in water contributes to the water stability of U-gels. To our knowledge, this is the first report presenting water-insoluble PAMPS hydrogels with 99.99% water content formed via entirely of H-bonds.

Table 1 also reveals that, as compared to the T-50 gel, an improvement in the gel mechanical performances is observable after applying a UV polymerization technique without deteriorating stretch at break, which remained above 1000%. The U-60 gel has the highest modulus E (65 ± 5 kPa) and fracture strength σ_f (114 ± 7 kPa) and sustains $1120 \pm 90\%$ elongations. However, all U-gels exhibited plastic deformation under load, which is undesirable in many applications of tough hydrogels. For instance, successive cyclic tensile tests conducted on U-gels with increasing maximum strain from 100 to 600% resulted in a permanent deformation after each unloading step that increased with increasing maximum strain (Figure S3). This plastic deformation indicates that the gel elasticity of the PAMPS network is insufficient to recover the original conformation. To eliminate plastic deformation and improve the elastic properties of the hydrogels, one may include a chemical cross-linker such as *N,N'*-methylenebis(acrylamide) (BAAM) in the monomer feed. However, experiments showed that even the addition of a small amount of BAAM significantly decreases both the stretchability and swelling capacity of PAMPS hydrogels without a considerable increase in the modulus and fracture stress (Figures S4 and S5). For instance, the addition of 0.1 mol % BAAM reduces the strain at break from 1800 to 250% and the swelling ratio m_{rel} from 880 to 94, whereas the modulus E slightly increases from 27 to 50 kPa. Calculations show that the contribution of H-bonds on the cross-link density of BAAM-cross-linked hybrid

hydrogels reduces to around 50% upon incorporation of 0.1 mol % BAAM, which could be the reason for their deteriorated mechanical properties (Figure S4). Another strategy to improve the mechanical strength of the hydrogels is to incorporate comonomer units into the PAMPS chains strengthening H-bonding interactions, which will be discussed in the next section.

Effect of DMAA as an H-Bonding Acceptor. *N,N*-dimethylacrylamide (DMAA) monomer with its strong H-bond acceptor properties is a good candidate to strengthen H-bonding interactions in PAMPS hydrogels. Polymers derived from DMAA are also attractive for building physical gels due to their ability to form hydrophobic associations.^{9,46,47} Further, we observed that DMAA could be solubilized in saturated aqueous solution of 60 wt % AMPS, which provided the formation of hydrogels with a high polymer content. By adding DMAA into 60 wt % AMPS solution, we were able to increase the total monomer concentration C_0 up to 80 wt %, during which the mole fraction of DMAA (x_{DMAA}) in the feed increased up to 0.74 (Table 1). In the following, AMPS/DMAA hydrogels are named as copolymer hydrogels, or as U- x/y , where x and y are the total monomer concentration C_0 and DMAA mole fraction x_{DMAA} in round numbers, respectively (Table 1).

Similar to U- x gels, copolymer gels were insoluble in water with a gel fraction W_g around unity, and they all exhibited large swelling ratios m_{rel} between 934 and 1622 in water (Table 1). An interesting point is that the incorporation of nonionic DMAA segments into the ionic PAMPS network up to a mole fraction of $x_{\text{DMAA}} = 0.74$ leads to an increase in the swelling ratio of the hydrogels. For instance, the purely ionic U-60 hydrogel exhibits a swelling ratio m_{rel} of 1013 ± 53 , whereas incorporation of 20 wt % nonionic DMAA segments into this hydrogel produces a hydrogel (U-70/0.5) with $m_{\text{rel}} = 1662 \pm 11$. This excess swelling of DMAA-containing hydrogels stands in contrast to the Flory–Rehner theory predicting that the equilibrium swelling degree is directly proportional to the charge density of hydrogels.⁴⁸ We attribute this behavior to the counterion condensation in ionic gels at high charge densities leading to the formation of “osmotically passive” counterions, which do not contribute to the swelling process.^{29,49–52} According to Manning’s theory,⁵³ if the distance A between two consecutive charges on the network chains reduces to the Bjerrum length Q , counterions in ionic hydrogels start to condense and reduce their ionic osmotic pressure in water. For PAMPS hydrogels swollen in water, the Bjerrum length Q is around 0.71 nm,²⁹ and the counterion distance A can be calculated as b/x_{AMPS} , where b is the bond length that is 0.25 nm for vinyl polymers, and $x_{\text{AMPS}} = 1 - x_{\text{DMAA}}$. The counterion distance A was calculated as 0.25, 0.46, and 0.66 nm for U-60, U-70/0.5, and U-75/0.6 hydrogels, respectively. Thus, incorporation of nonionic DMAA segments into PAMPS hydrogels increases the distance A between charged AMPS units, suppressing condensation of counterions and hence contributing to the swelling of the hydrogels in water.

Copolymer hydrogels could also be dissolved in urea solutions revealing that they are also formed solely via noncovalent bonds. However, the solubilization of the copolymer hydrogels in water required harsh conditions, for example, a high concentration of urea (7–10 M) and a long dissolution time under stirring (15 days). Figure 3 shows the shear rate dependence of the viscosity η and frequency dependences of the dynamic moduli G' and G'' of an aqueous

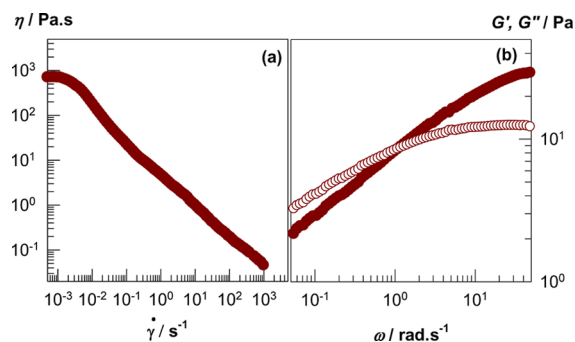


Figure 3. (a): Shear rate $\dot{\gamma}$ dependence of the viscosity η of 0.39 wt % U-75/0.6 solution. (b): Frequency ω dependences of G' (filled symbols) and G'' (open symbols) of the same solution. $\gamma = 0.1$.

0.39 wt % U-75/0.6 solution derived from the corresponding copolymer gel. The zero shear viscosity η_0 is 700 ± 40 Pa·s, which is 30-fold larger than that of the U-50 solutions. Moreover, the crossover frequency decreases from 2.6 to 1.1 $\text{rad}\cdot\text{s}^{-1}$, that is, the lifetime of physical bonds increases from 0.38 to 0.91 s upon incorporation of DMAA units in the hydrogel. The number-average molecular weight of the copolymer chains isolated from U-75/0.6 was measured as 1.4×10^6 $\text{g}\cdot\text{mol}^{-1}$ (Figure 2c), which is 2- and 170-fold larger than that of DMAA-free U-50 and T-50 hydrogels, respectively. The higher molecular weight of AMPS/DMAA copolymers as compared to PAMPS formed under identical conditions could be related to the hydrophobic associations between DMAA segments,⁵⁴ reduced propagation rate constant AMPS homopolymerization at high AMPS contents,⁵⁵ and favorable reactivity ratios of AMPS and DMAA during free radical polymerization.^{56,57} Thus, DMAA significantly contributes to the strength of the H-bonds in PAMPS hydrogels by increasing the length of their primary chains.

To gain more insight into the H-bonding interactions in the hydrogels, quantum mechanical calculations were carried out to study the nature of H-bonds between AMPS monomers, $(\text{AMPS})_2$, and AMPS/DMAA dimers. The calculations were conducted in the gas phase as well as in acidic aqueous medium with implicit and explicit water. AMPS has adjacent C=O and N–H bonds, which can be *trans* or *cis* to each other, where the latter conformation enables the formation of an intramolecular H-bond at a distance of 1.74 Å (Figure S6). AMPS in the gas phase possesses three acceptor and two donor groups, whereas upon incorporation of DMAA, the AMPS/DMAA dimer gains one more acceptor group (Figure S7). The H-bonding interaction energies between AMPS monomers and AMPS/DMAA dimers in the gas phase were calculated as -77.4 and -187.9 $\text{kJ}\cdot\text{mol}^{-1}$, respectively, revealing that the H-bonds formed between copolymer chains are much stronger than those formed between PAMPS chains (Table 2). In aqueous medium, $(\text{AMPS})_2$ and AMPS/DMAA dimers have four and two sulfonyl groups, respectively, and one hydronium hydrate ($\text{H}_3\text{O}^+\cdot\text{H}_2\text{O}$) per sulfonyl group. In the absence of counterions, $(\text{AMPS})_2$ dimers form one intermolecular H-bond between each other at a distance of 1.96 Å, whereas two intermolecular H-bonds at 1.92 and 2.34 Å distances are formed between AMPS/DMAA dimers, revealing stronger hydrogen bonding interactions between copolymers (Figure S8). The calculated intermolecular interaction energies for $(\text{AMPS})_2$ and AMPS/DMAA are $+487.9$ and $+145.6$ $\text{kJ}\cdot\text{mol}^{-1}$, respectively, that is, they are repulsive due to the negative

Table 2. BSSE-Corrected Intermolecular Interaction Energies of the Dimer Molecules Obtained at M062X/6-311+G(d,p) Level, in the Gas Phase, and with Implicit and Explicit Water

system	BSSE-corrected intermolecular interaction energy (kJ·mol ⁻¹)		
	gas phase	implicit water	explicit water
AMPS–AMPS	–77.4		
(AMPS) ₂ –(AMPS) ₂		+487.9	–28.0
AMPS/DMAA–AMPS/DMAA	–187.9	+145.6	–46.4
H ₂ O–H ₂ O	–23.8		between –15.1 and –19.7 ⁵⁸

charges, but less repulsive for the latter due to its lower negative charge. In the presence of H₃O₂⁺ counterions, the optimization of the structures suffered from convergence problems due to the highly mobile water molecules that can adapt different conformations very easily. We have observed that the negative charges on the sulfonfyl groups are distributed among the oxygen atoms bonded to the sulfur atom, and the positive charge on the hydronium ion is distributed over the adjacent water molecule coordinated via H-bonding to it. Between AMPS/DMAA dimers, two H-bonds form at distances between 1.9–2.4 Å, whereas no intermolecular bonds were observed between (AMPS)₂ dimers (Figure S9). Moreover, the intermolecular interaction energies for (AMPS)₂ and AMPS/DMAA dimers were calculated as –28.0 and –46.4 kJ·mol⁻¹, respectively (Table 2). The calculations thus confirm that the H-bonds between AMPS/DMAA copolymers are stronger than those between PAMPS polymers.

Mechanical and Self-Healing Properties. Figure 4 shows tensile stress–strain curves and the mechanical parameter of the hydrogels with mole fractions x_{DMAA} of DMAA between 0 and 0.74. Increasing x_{DMAA} up to 0.62, that is, increasing total monomer concentration C_0 from 60 to 75 wt %, significantly increases both the modulus E and the fracture stress σ_f of the hydrogels, while stretch at break ϵ_f remains still around 1000%. At $C_0 = 75$ wt %, E becomes 0.41 ± 0.02 MPa, which is in the range of the modulus of articular cartilage (0.31–0.80 MPa).⁵⁹ One may argue that the modulus increase with increasing x_{DMAA} is due to the simultaneous increase of the polymer content of hydrogels, rather than increasing effective cross-link density, that is, the formation of additional H-bonds between AMPS and DMAA units. To investigate this point, the cross-linking density of the hydrogels

was estimated from their Young's moduli E using the equation^{48,60}

$$E = 3\nu_e RT \quad (2)$$

where ν_e is the cross-link density, that is, the number of network chains per volume of gel; R and T are in their usual representations. Equation 2 assumes an affine deformation of the network chains, which is a reasonable assumption for the physical gels under study.¹¹ Because ν_e will increase with increasing C_0 , to eliminate the concentration effect, we calculated the cross-link density ν_e^{dry} per volume of dry polymer by $\nu_e^{\text{dry}} = \nu_e/\nu_2^0$, where ν_2^0 is the volume fraction of the cross-linked polymer in as-prepared hydrogels. Using the moduli E of the hydrogels (Figure 4b) together with the density of PAMPS (1.44 g·cm⁻³),²⁹ ν_e^{dry} was calculated using eq 2 and is plotted in Figure 4b against C_0 . Similar to the modulus increase, ν_e^{dry} significantly increases with C_0 up to 75 wt %, indicating that the incorporation of DMAA into PAMPS chains increases the number of noncovalent bonds acting as cross-links.

To further highlight the existence of a larger number of physical bonds in copolymer hydrogels as compared to PAMPS hydrogels, their large-strain behavior was investigated by cyclic mechanical tests. Figure 5a shows typical tensile cycles consisting of eight successive loading and unloading steps conducted on a U-75/0.6 copolymer gel specimen. The tests were carried out with increasing maximum strain ϵ_{max} up to 800% in eight steps, as indicated by the arrows. In contrast to pure PAMPS hydrogels exhibiting permanent deformation, the copolymer gels fully recover to their original sizes within 1 min after unloading (inset of Figure 5a, Figure S10). This behavior is also illustrated in Figure 6a and Figure S11, where the images of knotted and rod-shaped U-75/0.6 gel specimens are shown. After stretching the specimens to 800% elongation, they self-recover their original sizes within 1 min. Thus, DMAA significantly contributes to the elasticity of PAMPS hydrogels. Figure 5a also shows that, similar to PAMPS gels (Figure S3), each loading curve closely follows the previous loading, indicating quasi-reversibility of the cycles. The solid symbols in Figure 5b show the hysteresis energies U_{hys} of the copolymer hydrogel calculated from the area between the loading and unloading curves plotted against the maximum strain ϵ_{max} . For comparison, U_{hys} data of PAMPS hydrogels with C_0 between 50 and 60 wt % AMPS are also shown in the figure by the open symbols. Incorporation of DMAA units significantly increases the hysteresis energy, that is, the number of bonds reversibly broken under strain. For instance, at $\epsilon_{\text{max}} = 600\%$, the U_{hys} of a

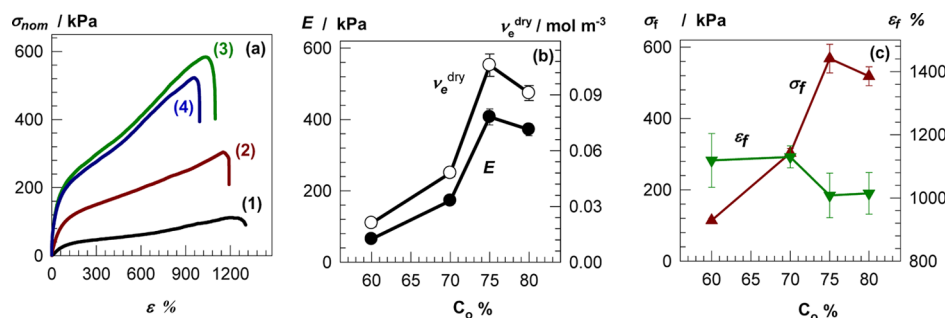


Figure 4. (a): Tensile stress–strain curves of copolymer hydrogels. The concentration C_0 and the mole fraction x_{DMAA} of DMAA in the comonomer feed (in parentheses) for the curves 1, 2, 3, and 4 are 60(0), 70(0.46), 75(0.62), and 80(0.74) wt %, respectively. (b, c): Young's modulus E , the crosslink density ν_e^{dry} , tensile strength σ_f , and stretch at break ϵ_f of the hydrogels plotted against C_0 .

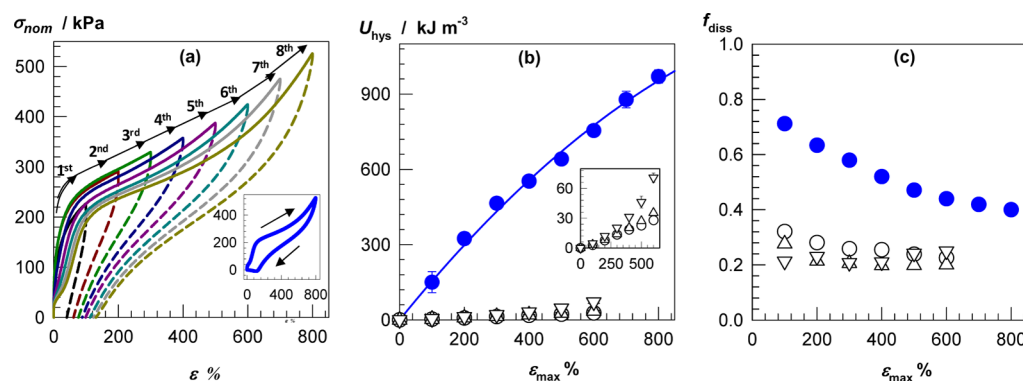


Figure 5. (a): Cyclic tensile tests conducted on the U-75/0.6 hydrogel with increasing maximum strain ϵ_{\max} from 100 to 800% in eight steps. Strain rate = 5 min^{-1} . Loading curves are indicated by arrows. The inset shows the last loading/unloading cycle with $\epsilon_{\max} = 800\%$. (b, c): U_{hys} and f_{diss} of U-75/0.6 hydrogels (solid blue circles) plotted against ϵ_{\max} . The line in (b) is the best fit to the experimental data. For comparison, U_{hys} and f_{diss} data of U-gels prepared at $C_0 = 50, 55,$ and $60 \text{ wt } \%$ are also shown by open circles and upward and downward triangles, respectively.

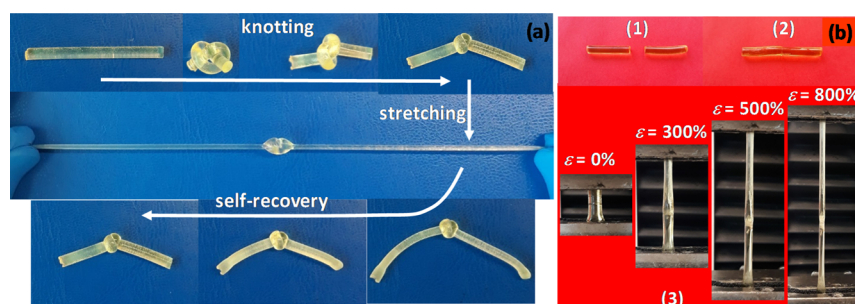


Figure 6. (a): Self-recovery behavior of knotted U-75/0.6 gel specimens after stretching. (b): Self-healing of U-75/0.6 gel specimens at $23 \pm 2 \text{ }^\circ\text{C}$ after 24 h (1, 2) and tensile testing after healing to 800% stretch ratio (3).

copolymer hydrogel is 10 to 30-fold larger than that of PAMPS hydrogels (755 vs $28\text{--}70 \text{ kJ}\cdot\text{m}^{-3}$).

The ratio of dissipated energy to the loading energy (f_{diss}), that is, the amount of energy dissipated per loading energy can be regarded as a parameter presenting the extent of energy dissipation under a constant external load.⁴ We calculated f_{diss} from the ratio of U_{hys} to the loading energy, that is, the area under the loading curve. Figure 5c shows f_{diss} data of the U-75/0.6 copolymer gel (solid symbols) and U-gels with C_0 between 50 and 60 wt % (open symbols) plotted against ϵ_{\max} . For the U-gels prepared without DMAA, this fraction is $25 \pm 4\%$ and almost independent on ϵ_{\max} or AMPS concentration, while for U-75/0.6, f_{diss} is close to 80% at low strains and gradually decreases with increasing strain, approaching to a limiting value of 40% at large strains. This finding also reveals a significant increase of the number of reversible bonds in PAMPS hydrogels after incorporation of DMAA segments.

U_{hys} can be regarded as the sum of the dissociation energies of intermolecular noncovalent bonds broken down during the cyclic tests, that is¹¹

$$U_{\text{hys}} = U_{\text{xl}}\nu_e f_v \quad (3)$$

where U_{xl} is the average dissociation energy of intermolecular bonds; ν_e is, as defined above, the cross-link density of the hydrogel, that is, the total number of such bonds; and f_v is the fraction of bonds broken during the tensile cycle. The fraction f_v of broken bonds depends on the strain, and hence it increases with increasing strain ϵ_{\max} . Thus, the initial slope of U_{hys} versus ϵ_{\max} plots can be written as

$$\lim_{\epsilon \rightarrow 0} \left(\frac{\partial U_{\text{hys}}}{\partial \epsilon_{\max}} \right) = U_{\text{xl}}\nu_e \quad (4)$$

The solid curve in Figure 5b is the best fit to the U_{hys} versus ϵ_{\max} data, yielding an initial slope of $156 \pm 6 \text{ kJ}\cdot\text{m}^{-3}$. From the modulus $E = 407 \pm 22 \text{ kPa}$ for the U-75/0.6 hydrogel, we calculated its cross-link density ν_e using eq 2 as $55 \pm 3 \text{ mol}\cdot\text{m}^{-3}$. Substituting these values into eq 4, the average dissociation energy U_{xl} of the noncovalent bonds in the hydrogel was estimated as $2.9 \pm 0.2 \text{ kJ}\cdot\text{mol}^{-1}$. Because of the existence of a large number of H-bonds of varying strengths, one may expect that the breaking of H-bonds under strain occurs gradually so that the calculated dissociation energy corresponds to the weak H-bonds broken under 800% strain.^{61,62} Thus, copolymer hydrogels are solely formed by H-bonding interactions between AMPS/AMPS and AMPS/DMAA segments.

The quasi-reversible manner of dissociation of H-bonds in the hydrogels under stress suggests their self-healing abilities. The images in Figure 6b show photographs of a gel specimen after cutting into two parts (1) and after healing at $23 \pm 2 \text{ }^\circ\text{C}$ by pushing the cut surfaces together for 24 h (2). The repaired sample could withstand 900% strain, which is close to that of the virgin sample (image 3). To quantify the self-healing ability of the hydrogels, they were first cut into two parts, and the cut surfaces were then pushed together at $23 \pm 2 \text{ }^\circ\text{C}$ to induce healing. Figure 7a shows the stress–strain curves of the virgin and healed U-75/0.6 gel specimens for various times. Healing efficiencies ϵ_h with respect to the modulus E , fracture strain σ_f and fracture strain ϵ_f are shown in Figure 7b plotted against the healing time. After a healing time of 24 h, the U-75/0.6

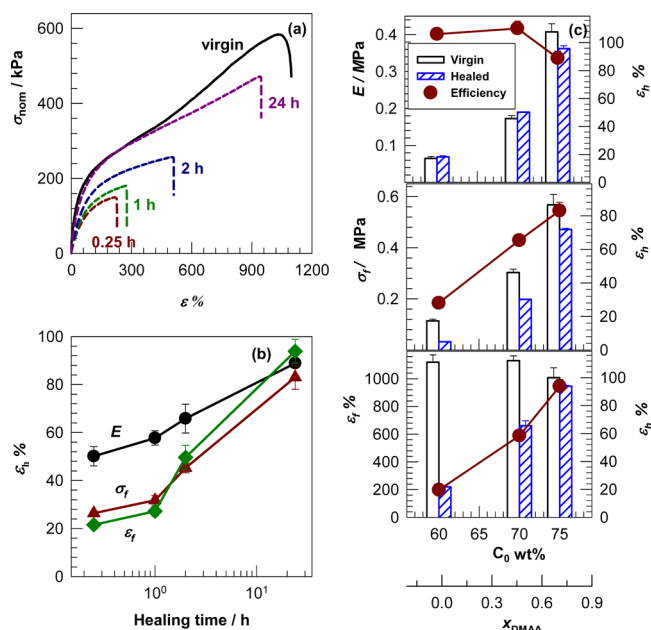


Figure 7. (a): Stress–strain curves of the virgin (solid curve) and healed U-75/0.6 hydrogels (dashed curves) at various healing times at 23 ± 2 °C. (b): Healing efficiencies of the U-75/0.6 hydrogel with respect to the modulus E , fracture stress σ_f and strain ϵ_f plotted against the healing time. (c): The modulus E , fracture stress σ_f and strain ϵ_f of virgin and healed hydrogels, and the corresponding healing efficiencies ϵ_h plotted against C_0 and x_{DMAA} . Healing time = 24 h.

hydrogel sustains to a stretch ratio of 900 ± 30 , which is close to that of the virgin hydrogel (1000 ± 50). Moreover, the healing efficiency is significantly time-dependent, and the highest healing efficiencies with respect to E , σ_f and ϵ_f could be obtained after 24 h of healing time.

Figure 7c shows the mechanical parameters E , σ_f and ϵ_f of virgin and healed hydrogels together with the corresponding healing efficiencies ϵ_h as functions of C_0 and x_{DMAA} . All hydrogels prepared with or without DMAA exhibit around 100% healing efficiency with respect to the modulus, revealing recovery of the original microstructure. However, healing efficiencies with respect to the fracture stress and fracture strain monotonically increase with the amount of DMAA segments in the hydrogels. For instance, the U-60 gel prepared

at 60 wt % AMPS without DMAA shows healing efficiencies of 28 and 20% with respect to the fracture stress and strain, respectively. Even after a healing time of 71 h, only 23% healing could be obtained in the fracture stress of healed gel specimens. However, incorporation of DMAA at a level of $x_{\text{DMAA}} = 0.74$ increases the healing efficiency to 80–90% after 24 h of healing, revealing the significant contribution of DMAA segments to the recovery of the ultimate mechanical properties.

The mechanical performances of the physical gels discussed above were determined in their as-prepared states with water contents between 20–50 wt %. It seems challenging to observe similar extraordinary mechanical properties in their equilibrium swollen states with water contents of around 99.99%. However, this contradicts the finite extensibility of polymer chains, as schematically illustrated in Figure 8a. Here, the end-to-end distances of a network chain in as-prepared and equilibrium swollen states and at the point of fracture are denoted as R_0 , R_s , and R_f , respectively. Thus, the deformation ratio λ_f at break of as-prepared hydrogels can be written as $\lambda_f = R_f/R_0$, whereas the chain expansion at the equilibrium degree of swelling is given by $\alpha_s = R_s/R_0$. Although λ_f and α_s are fixed quantities for a given hydrogel, the elongation ratio at break of the hydrogels in their equilibrium swollen states ($\lambda_{s,f}$) is a dependent quantity given by

$$\lambda_{s,f} = \frac{\lambda_f}{\alpha_s} \quad (5)$$

Because $\alpha_s \cong (m_{\text{rel}})^{1/3}$ and $\lambda_f = \epsilon_f + 1$, one may estimate $\lambda_{s,f}$ of swollen hydrogels using eq 5 together with the values of m_{rel} and ϵ_f of as-prepared hydrogels (Table 1). For U-70/0.5, U-75/0.6, and U-80/0.7 hydrogels, their elongation ratios $\lambda_{s,f}$ at break in swollen states were calculated as 1.04 ± 0.03 , 1.10 ± 0.08 , and 1.15 ± 0.07 , respectively, revealing that they will fracture below 15% strain. Thus, as compared to around 1000% stretchability of as-prepared hydrogels, the stretchability in their swollen states will significantly reduce due to the almost fully stretched conformation of the network chains. The tensile tests conducted on swollen gel specimens indeed showed that they all fracture in a brittle fashion at the start of the mechanical tests. Figure 8b shows compressive stress–strain curves of swollen and as-prepared hydrogels prepared at three different initial monomer concentrations C_0 , while the

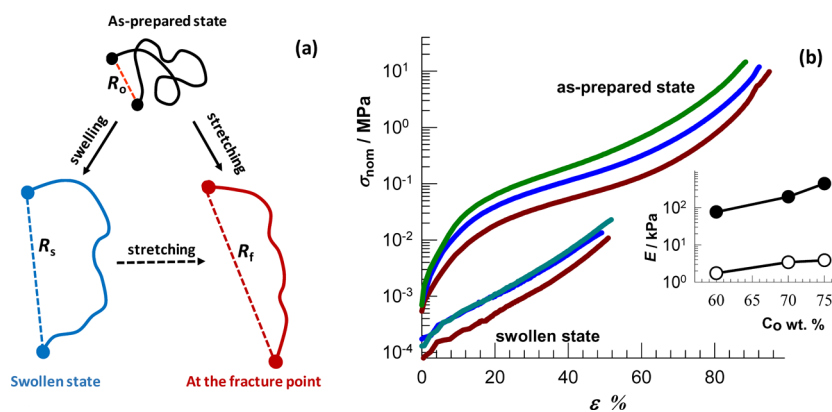


Figure 8. (a): Scheme of a network chain during swelling and stretching. R_0 , R_s , and R_f are end-to-end distances in the as-prepared state, swollen state, and at the fracture point, respectively. (b): Compressive stress–strain curves of copolymer hydrogels in swollen and as-prepared states. $C_0 = 60$ (dark red), 70 (blue), and 75 wt % (dark green). Inset shows Young's modulus E of the hydrogels in swollen (open symbols) and as-prepared states (solid symbols) plotted against C_0 .

inset shows the Young's moduli E of swollen (open symbols) and as-prepared hydrogels (solid symbols) plotted against C_0 . As compared to the 80–93% compressibility of as-prepared hydrogels, swollen hydrogels rupture under 50% compression. Moreover, swelling causes a Young's modulus drop of two orders of magnitude, indicating an occurrence of significant internal damage at 5–15% strains due to highly stretched conformation of the network chains. These results also indicate that the swollen copolymer hydrogels are a good candidate as sacrificial bonds, that is, as the first-network component of double-network hydrogels to create less swollen but mechanically stronger hydrogels.⁶³

CONCLUSIONS

PAMPS hydrogels are attractive materials for various application areas due to their pH-independent large swelling capacities. However, their chemically cross-linked network structure prevents dissipation of energy under load, leading to their fracture under low strain. We presented here, for the first-time, superabsorbent PAMPS hydrogels formed solely by H-bonding interactions that are stable in water. UV polymerization of AMPS at 23 ± 2 °C in aqueous solutions without a chemical cross-linker produces water-insoluble, highly stretchable physical hydrogels with swelling capacities exceeding 1000 times their original mass. The stability of the physical gels in water is attributed to the high molecular weight of their PAMPS primary chains contributing to the H-bonding cooperativity. The molecular weight of PAMPS chains isolated from the hydrogels is around two orders of magnitude higher than those of thermal polymerized ones. Incorporation of DMAA segments into the physical gels further increases the molecular weight of the primary chains, leading to enhanced mechanical strength of the hydrogels. PAMPS/DMAA hydrogels in their as-prepared states exhibit a high modulus (up to 0.41 MPa), tensile fracture stress (up to 0.57 MPa), and high stretchability (~ 1000) together with an extraordinary swelling capacity (up to ~ 1700 g·g⁻¹) and complete self-healing efficiency. We also show that the network chains of the hydrogels in an equilibrium swollen state are in an almost fully stretched conformation due to the significant swelling pressure. As a consequence, swelling causes a significant drop in both stretchability and the modulus of the hydrogels.

ASSOCIATED CONTENT

Supporting Information

The Supporting Information is available free of charge on the ACS Publications website at DOI: 10.1021/acs.macromol.9b00032.

Supplementary characterization data including swelling, rheological, and mechanical test results (PDF)

AUTHOR INFORMATION

Corresponding Author

*E-mail: okayo@itu.edu.tr.

ORCID

Mine Yurtsever: 0000-0001-6504-7182

Oguz Okay: 0000-0003-2717-4150

Author Contributions

The manuscript was written through contributions of all authors. All authors have given approval to the final version of the manuscript.

Notes

The authors declare no competing financial interest.

ACKNOWLEDGMENTS

E.S. thanks TUBITAK-BIDEB for a Ph.D. scholarship. O.O. thanks the Turkish Academy of Sciences (TUBA) for the partial support. M.Y. acknowledges the computing resources provided by the National Center for High Performance Computing of Turkey (UHeM) under grant number 5004452017.

REFERENCES

- (1) Okay, O. General properties of hydrogels, in: Gerlach, G.; Arndt, K. F. (eds.), *Hydrogel sensors and actuators. Springer Series on Chemical Sensors and Biosensors* Vol. 6, Springer Berlin Heidelberg, 2009, pp. 1–14.
- (2) Ahagon, A.; Gent, A. N. Threshold fracture energies for elastomers. *J. Polym. Sci. Polym. Phys. Ed.* **1975**, *13*, 1903–1911.
- (3) Brown, H. R. A model of the fracture of double network gels. *Macromolecules* **2007**, *40*, 3815–3818.
- (4) Cretton, C. 50th Anniversary perspective: Networks and gels: Soft but dynamic and tough. *Macromolecules* **2017**, *50*, 8297–8316.
- (5) Phadke, A.; Zhang, C.; Arman, B.; Hsu, C.-C.; Mashelkar, R. A.; Lele, A. K.; Tauber, M. J.; Arya, G.; Varghese, S. Rapid self-healing hydrogels. *Proc. Natl. Acad. Sci. U. S. A.* **2012**, *109*, 4383–4388.
- (6) Zhang, H.; Xia, H.; Zhao, Y. Poly(vinyl alcohol) hydrogel can autonomously self-heal. *ACS Macro Lett.* **2012**, *1*, 1233–1236.
- (7) Cui, J.; del Campo, A. Multivalent H-bonds for self-healing hydrogels. *Chem. Commun.* **2012**, *48*, 9302–9304.
- (8) Liu, J.; Song, G.; He, C.; Wang, H. Self-healing in tough graphene oxide composite hydrogels. *Macromol. Rapid Commun.* **2013**, *34*, 1002–1007.
- (9) Uzumcu, A. T.; Guney, O.; Okay, O. Highly stretchable DNA/clay hydrogels with self-healing ability. *ACS Appl. Mater. Interfaces* **2018**, *10*, 8296–8306.
- (10) Gong, Z.; Zhang, G.; Zeng, X.; Li, J.; Li, G.; Huang, W.; Sun, R.; Wong, C. High-strength, tough, fatigue resistant, and self-healing hydrogel based on dual physically cross-linked network. *Appl. Mater. Interfaces* **2016**, *8*, 24030–24037.
- (11) Tuncaboylu, D. C.; Sahin, M.; Argun, A.; Oppermann, W.; Okay, O. Dynamics and large strain behavior of self-healing hydrogels with and without surfactants. *Macromolecules* **2012**, *45*, 1991–2000.
- (12) Okay, O. Self-healing hydrogels formed via hydrophobic interactions. *Adv. Polym. Sci.* **2015**, *268*, 101–142.
- (13) Bilici, C.; Can, V.; Nöchel, U.; Behl, M.; Lendlein, A.; Okay, O. Melt-processable shape-memory hydrogels with self-healing ability of high mechanical strength. *Macromolecules* **2016**, *49*, 7442–7449.
- (14) Deringer, V. L.; Englert, U.; Dronskowski, R. Covalency of hydrogen bonds in solids revisited. *Chem. Commun.* **2014**, *50*, 11547–11549.
- (15) Yanagisawa, Y.; Nan, Y.; Okuro, K.; Aida, T. Mechanically robust, readily repairable polymers via tailored noncovalent cross-linking. *Science* **2018**, *359*, 72–76.
- (16) Perrin, C. L.; Nielson, J. B. Strong hydrogen bonds in chemistry and biology. *Annu. Rev. Phys. Chem.* **1997**, *48*, 511–544.
- (17) Dai, X.; Zhang, Y.; Gao, L.; Bai, T.; Wang, W.; Cui, Y.; Liu, W. A mechanically strong, highly stable, thermoplastic, and self-healable supramolecular polymer hydrogel. *Adv. Mater.* **2015**, *27*, 3566–3571.
- (18) Tang, L.; Liu, W.; Liu, G. High-strength hydrogels with integrated functions of H-bonding and thermoresponsive surface-mediated reverse transfection and cell detachment. *Adv. Mater.* **2010**, *22*, 2652–2656.
- (19) Gao, H.; Wang, N.; Hu, X.; Nan, W.; Han, Y.; Liu, W. Double hydrogen-bonding pH-sensitive hydrogels retaining high-strengths over a wide pH range. *Macromol. Rapid Commun.* **2013**, *34*, 63–68.
- (20) Guo, M.; Pitet, L. M.; Wyss, H. M.; Vos, M.; Dankers, P. Y. W.; Meijer, E. W. Tough stimuli-responsive supramolecular hydrogels

with hydrogen-bonding network junctions. *J. Am. Chem. Soc.* **2014**, *136*, 6969–6977.

(21) Jeon, I.; Cui, J.; Illeperuma, W. R. K.; Aizenberg, J.; Vlassak, J. J. Extremely stretchable and fast self-healing hydrogels. *Adv. Mater.* **2016**, *28*, 4678–4683.

(22) Zhang, Y.; Li, Y.; Liu, W. Dipole-dipole and H-bonding interactions significantly enhance the multifaceted mechanical properties of thermoresponsive shape memory hydrogels. *Adv. Funct. Mater.* **2015**, *25*, 471–480.

(23) Hu, X.; Vatankhah-Varnoosfaderani, M.; Zhou, J.; Li, Q.; Sheiko, S. S. Weak hydrogen bonding enables hard, strong, tough, and elastic hydrogels. *Adv. Mater.* **2015**, *27*, 6899–6905.

(24) Ding, H.; Zhang, X. N.; Zheng, S. Y.; Song, Y.; Wu, Z. L.; Zheng, Q. Hydrogen bond reinforced poly(1-vinylimidazole-co-acrylic acid) hydrogels with high toughness, fast self-recovery, and dual pH-responsiveness. *Polymer* **2017**, *131*, 95–103.

(25) Zhang, X. N.; Wang, Y. J.; Sun, S.; Hou, L.; Wu, P.; Wu, Z. L.; Zheng, Q. A tough and stiff hydrogel with tunable water content and mechanical properties based on the synergistic effect of hydrogen bonding and hydrophobic interaction. *Macromolecules* **2018**, *51*, 8136–8146.

(26) Fisher, L. W.; Sochor, A. R.; Tan, J. S. Chain characteristics of poly(2-acrylamido-2-methylpropanesulfonate) polymers. 1. light-scattering and intrinsic-viscosity studies. *Macromolecules* **1977**, *10*, 949–954.

(27) Tong, Z.; Liu, X. Swelling equilibria and volume phase transition in hydrogels with strongly dissociating electrolytes. *Macromolecules* **1994**, *27*, 844–848.

(28) Liu, X.; Tong, Z.; Hu, O. Swelling equilibria of hydrogels with sulfonate groups in water and in aqueous salt solutions. *Macromolecules* **1995**, *28*, 3813–3817.

(29) Durmaz, S.; Okay, O. Acrylamide/2-acrylamido-2-methylpropane sulfonic acid sodium salt-based hydrogels: synthesis and characterization. *Polymer* **2000**, *41*, 3693–3704.

(30) Gundogan, N.; Melekaslan, D.; Okay, O. Rubber elasticity of poly(N-isopropylacrylamide) gels at various charge densities. *Macromolecules* **2002**, *35*, 5616–5622.

(31) Su, E.; Okay, O. Hybrid cross-linked poly(2-acrylamido-2-methyl-1-propanesulfonic acid) hydrogels with tunable viscoelastic, mechanical and self-healing properties. *React. Funct. Polym.* **2018**, *123*, 70–79.

(32) Boonkaew, B.; Barber, P. M.; Rengpipat, S.; Supaphol, P.; Kempf, M.; He, J.; John, V. T.; Cuttle, L. Development and Characterization of a Novel, Antimicrobial, Sterile Hydrogel Dressing for Burn Wounds: Single-Step Production with gamma irradiation creates silver nanoparticles and radical polymerization. *J. Pharm. Sci.* **2014**, *103*, 3244–3253.

(33) Yang, C.; Liu, Z.; Chen, C.; Shi, K.; Zhang, L.; Ju, X.-J.; Wang, W.; Xie, R.; Chu, L. Y. Reduced graphene oxide-containing smart hydrogels with excellent electro-response and mechanical properties for soft actuators. *ACS Appl. Mater. Interfaces* **2017**, *9*, 15758–15767.

(34) Jones, A.; Vaughan, D. Hydrogel dressings in the management of a variety of wound types: a review. *J. Orthop. Nurs.* **2005**, *9*, S1–11.

(35) Gong, J. P.; Kurokawa, T.; Narita, T.; Kagata, G.; Osada, Y.; Nishimura, G.; Kinjo, M. Synthesis of hydrogels with extremely low surface friction. *J. Am. Chem. Soc.* **2001**, *123*, 5582–5583.

(36) Nalampang, K.; Panjakha, R.; Molloy, R.; Tighe, B. J. Structural effects in photopolymerized sodium AMPS hydrogels crosslinked with poly(ethylene glycol) diacrylate for use as burn dressings. *J. Biomater. Sci., Polym. Ed.* **2013**, *24*, 1291–1304.

(37) Xing, X.; Li, L.; Wang, T.; Ding, Y.; Liu, G.; Zhang, G. A self-healing polymeric material: from gel to plastic. *J. Mater. Chem. A* **2014**, *2*, 11049–11053.

(38) Kazantsev, O. A.; Igolkin, A. V.; Shirshin, K. V.; Kuznetsova, N. A.; Spirina, A. N.; Malyshev, A. P. Spontaneous polymerization of 2-acrylamido-2-methylpropanesulfonic acid in acidic aqueous solutions. *Russ. J. Appl. Chem.* **2002**, *75*, 465–469.

(39) Carreau, P. J. Rheological equations from molecular network theories. *Trans. Soc. Rheol.* **1972**, *16*, 99–127.

(40) Argun, A.; Can, V.; Altun, U.; Okay, O. Non-ionic double and triple network hydrogels of high mechanical strength. *Macromolecules* **2014**, *47*, 6430–6440.

(41) Song, G.; Zhang, L.; He, C.; Fang, D. C.; Whitten, P. G.; Wang, H. Facile fabrication of tough hydrogels physically cross-linked by strong cooperative hydrogen bonding. *Macromolecules* **2013**, *46*, 7423–7435.

(42) Kříž, J.; Dybal, J.; Brus, J. Cooperative hydrogen bonds of macromolecules. 2. Two-dimensional cooperativity in the binding of poly(4-vinylpyridine) to poly(4-vinylphenol). *J. Phys. Chem. B* **2006**, *110*, 18338–18346.

(43) Kříž, J.; Dybal, J. Cooperative hydrogen bonds of macromolecules. 3. A model study of the proximity effect. *J. Phys. Chem. B* **2007**, *111*, 6118–6126.

(44) Han, S.; Cao, S.; Wang, Y.; Wang, J.; Xia, D.; Xu, H.; Zhao, X.; Lu, J. R. Self-assembly of short peptide amphiphiles: The cooperative effect of hydrophobic interaction and hydrogen bonding. *Chem. – Eur. J.* **2011**, *17*, 13095–13102.

(45) Nowick, J. S. Exploring β -sheet structure and interactions with chemical model systems. *Acc. Chem. Res.* **2008**, *41*, 1319–1330.

(46) Uemura, Y.; McNulty, J.; Macdonald, P. M. Associative behavior and diffusion coefficients of hydrophobically modified poly(N,N-dimethylacrylamides). *Macromolecules* **1995**, *28*, 4150–4158.

(47) Relógio, P.; Martinho, J. M. G.; Farinha, J. P. S. Effect of surfactant on the intra- and intermolecular association of hydrophobically modified poly(N,N-dimethylacrylamide). *Macromolecules* **2005**, *38*, 10799–10811.

(48) Flory, P. J. *Principles of Polymer Chemistry*; Cornell University Press: Ithaca, NY, 1953.

(49) Khokhlov, A. R.; Kramarenko, E. Y. Polyelectrolyte/ionomer behavior in polymer gel collapse. *Macromol. Theory Simul.* **1994**, *3*, 45–59.

(50) Zeldovich, K. B.; Khokhlov, A. R. Osmotically active and passive counterions in inhomogeneous polymer gels. *Macromolecules* **1999**, *32*, 3488–3494.

(51) Okay, O.; Durmaz, S. Charge density dependence of elastic modulus of strong polyelectrolyte hydrogels. *Polymer* **2002**, *43*, 1215–1221.

(52) Melekaslan, D.; Okay, O. Swelling of strong polyelectrolyte hydrogels in polymer solutions: Effect of ion pair formation on the polymer collapse. *Polymer* **2000**, *41*, 5737–5747.

(53) Manning, G. S. Limiting laws and counterion condensation in polyelectrolyte solutions I. Colligative properties. *J. Chem. Phys.* **1969**, *51*, 924–933.

(54) Morishima, Y.; Nomura, S.; Ikeda, T.; Seki, M.; Kamachi, M. Characterization of unimolecular micelles of random copolymers of sodium 2-(acrylamido)-2-methylpropanesulfonate and methacrylamides bearing bulky hydrophobic substituents. *Macromolecules* **1995**, *28*, 2874–2881.

(55) Beuermann, S.; Buback, M.; Hesse, P.; Junkers, T.; Lacić, I. Free-radical polymerization kinetics of 2-acrylamido-2-methylpropanesulfonic acid in aqueous solution. *Macromolecules* **2006**, *39*, 509–516.

(56) Scott, A.; Riahinezhad, M.; Penlidis, A. Optimal design for reactivity ratio estimation: A comparison of techniques for AMPS/acrylamide and AMPS/acrylic acid copolymerizations. *Processes* **2015**, *3*, 749–768.

(57) Pooley, S. A.; Rivas, B. L.; Cárcamo, A. L.; Pizarro, G. D. C. Hydrogels from N,N'-dimethylacrylamide-co-2-acrylamido-2-methyl-1-propanesulfonic acid with salt-, temperature- and pH-responsiveness properties. *J. Chil. Chem. Soc.* **2008**, *53*, 1483–1489.

(58) Mukhopadhyay, A.; Cole, W. T. S.; Saykally, R. J. The water dimer I: Experimental characterization. *Chem. Phys. Lett.* **2015**, *633*, 13–26.

(59) Baker, M. I.; Walsh, S. P.; Schwartz, Z.; Boyan, B. D. A review of polyvinyl alcohol and its uses in cartilage and orthopedic applications. *J. Biomed. Mater. Res. B Appl. Biomater.* **2012**, *100B*, 1451–1457.

(60) Treloar, L. R. G. *The Physics of Rubber Elasticity*; University Press: Oxford, 1975.

(61) Klotz, I. M. Solvent water and protein behavior: View through a retroscope. *Protein Sci.* **1993**, *2*, 1992–1999.

(62) Williams, D. H.; Searle, M. S.; Mackay, J. P.; Gerhard, U.; Maplestone, R. A. Toward an estimation of binding constants in aqueous solution: Studies of associations of vancomycin group antibiotics. *Proc. Natl. Acad. Sci. U. S. A.* **1993**, *90*, 1172–1178.

(63) Gong, J. P.; Katsuyama, Y.; Kurokawa, T.; Osada, Y. Double-network hydrogels with extremely high mechanical strength. *Adv. Mater.* **2003**, *15*, 1155–1158.